Optical Performance of Commercial Liquid Lens Assemblies in Microgravity

Shreeyam Kacker[a,*], **Kerri L. Cahoy**[a]
[a]Massachusetts Institute of Technology, Space Telecommunications, Astronomy and Radiation Laboratory, Department of Aeronautics and Astronautics, Cambridge, MA 02139, United States

Abstract. Liquid lenses have been utilized in various applications due to their low size, weight, power, and cost. They have potential for use in space applications such as focus compensation, optical communications, and imaging systems. However, liquid lenses have not yet been evaluated for us in space environment. This work focuses on characterizing operational differences of commercially available liquid lenses from Corning Varioptic and Optotune between Earth gravity, microgravity, and hypergravity environments. Results show a linear drift in tip/tilt of 0.79 mrad and 4.13 mrad going from 1 g to 0 g for the Corning Varioptic A-39N0 lens and Optotune EL-16-40-TC-VIS lenses respectively, with lower optical aberrations in microgravity. Additionally, focusing power increases going from 1 g to 0 g by 0.059 D for the Corning Varioptic lenses and 0.039 D for the Optotune lenses. This work is part of a wider space environment study showing that Corning Varioptic and Optotune's commercial liquid lenses withstand thermal vacuum, typical low Earth orbit ionizing radiation exposure, and effectively handle high-intensity laser power in a vacuum without significant damage.

Keywords: Liquid lens, space optics, microgravity, beam steering, optical communications, small satellites.

*Shreeyam Kacker, E-mail: shreeyam@mit.edu

1 Introduction

Liquid lenses are compact, nonmechanical focus-tunable lenses that use a liquid to change their focal length. Due to their low size, weight, power, and cost (SWaP-C) they are attractive for space applications, where they could be used for focus compensation, optical communications, and more. However, liquid lenses, have not been fully evaluated for use in the space environment. Previous work has subjected liquid lenses to thermal vacuum (TVAC) testing,[1,2] but other space environment tests such as ionizing radiation and microgravity has not yet been conducted. This work presents results using commercially available liquid lenses from Corning Varioptic and Optotune on a microgravity flight to characterize differences in operation between Earth gravity and microgravity. Microgravity testing is especially important, as the optical fluid sags in gravity causing increased wavefront error and aberrations.[3]

This work is part of development for the Miniature Optical Steered Antenna for Intersatellite Communication (MOSAIC) project which aims to utilize liquid lenses for a hemispherically steering lasercom terminal for small satellites, for which reliable operation in the space environment required.[1,2,4,5] The MOSAIC project aims to utilize liquid lens arrays for beam steering and laser communication on small satellites. The project seeks to construct a compact, nonmechanical lasercom transceiver with integrated beam steering for small satellites using liquid lenses. The transceiver design is based on a previous design by Zohrabi[6] utilizing a single on-axis lens for divergence control and an additional two lenses offset in x and y for 2D steering, initially proposed for LIDAR. Additionally, this work is part of a broader space environment evaluation effort including ionizing radiation testing and vacuum power handling performance, for which more details can be found in the full study by Kacker[5] – in summary, commercial liquid lenses from Corning Varioptic and Optotune perform well during TVAC testing, do not show gross discoloration when exposed to ionizing radiation equivalent to 10 years of low Earth orbit, and can handle over 2 W of laser power in vacuum

without damage.

2 Background

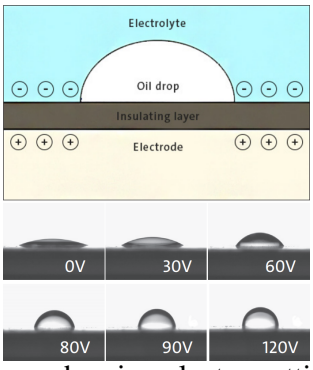

Fig 1: Diagram showing electrowetting principle of operation for Corning Varioptic lenses.[7]

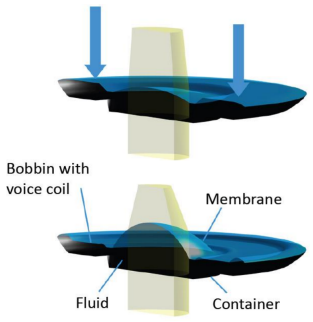

Fig 2: Diagram showing pressure based principle of operation for Optotune lenses.[3]

Liquid lenses have applications in machine vision,[3,7] phone cameras,[8] microscopy,[9] optical communications[10–14] and more due to their compactness and depending on the lens technology, low power. Optotune and Corning Varioptic are the two main companies making liquid lenses, each producing lenses with different operating principles. Corning Varioptic's liquid lenses employ electrowetting technology, where an applied electric field causes an oil droplet's contact angle with an insulator to change,[7] whereas Optotune's lenses function based on pressure, with a voice coil causing fluid to displace into the center of a membrane.[3] Diagrams of how Corning Varioptic's and Optotune's lenses work are shown in Fig. 1 and Fig. 2 respectively.

For satellite lasercom terminals, evaluating liquid lens performance in the space environment is important, including zero gravity testing. Previous work has shown that liquid lenses can survive and operate in other space environment conditions, including thermal vacuum testing[1,2] However, because liquid lenses use liquids to be focus tune-able, they experience a higher wavefront error and aberrations in the presence of gravity, with the Optotune lenses used in this study having an increased wavefront error of 50 nm[3] in Earth gravity conditions, measured by placing the lens in different orientations. Characterizing liquid lens performance under zero gravity conditions is crucial for space applications.

Previous work on evaluating the effects of gravity on liquid lenses has been conducted by changing the lens orientation, but this technique cannot eliminate the effects of gravity entirely.[15] This work presents zero gravity data from parabolic aircraft testing in order to understand the effects on optical performance.

3 Approach

3.1 Experimental Setup

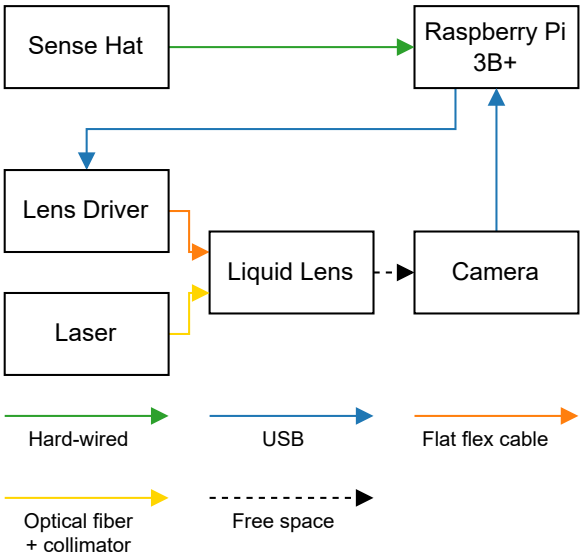

Fig 3: Block diagram of experiment components.

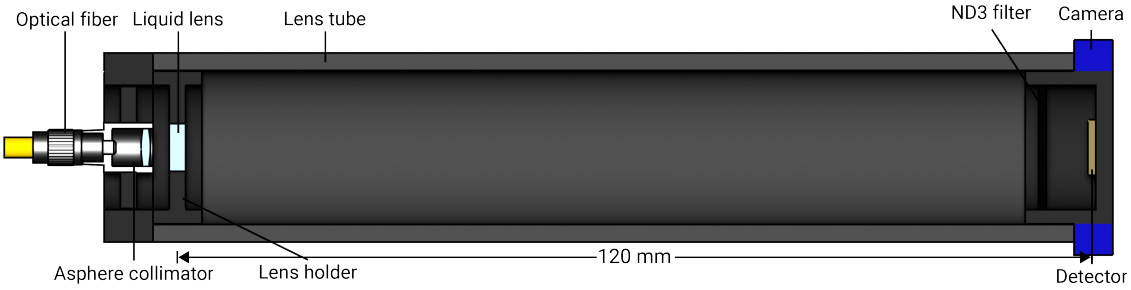

Fig 4: Diagram of single optical train in experimental setup.

Table 1: List of hardware used in experiment.

Device	**Property**	**Value**
Liquid Lens	Model (Corning Varioptic) Model (Optotune)	A-39N0 EL-16-40-TC-VIS-20D
Laser	Type Wavelength	1 mW Fiber Tester 633 nm
Collimator	Model Wavelength $1/e^2$ Diameter	Thorlabs F220FC-B 633 nm 2.1 mm
Camera	Make Model Pixel Pitch Binning Resolution Bit depth	Matrix Vision mvBlueFox-IGC 205v 2.2 µm 2×2 2592×1944 10 bit
Raspberry Pi	Model Hat	3B+ Sense Hat

The experiment consists of two independent optical trains, each operated by a dedicated Raspberry Pi. One optical train is for the Corning Varioptic lens, while the other is dedicated for the Optotune lens. A block diagram of one of these optical trains is shown in Fig. 3, and a diagram of the optical components is shown in Fig. 4, with further details about the hardware used in the experiment given in Table 1. A photograph of the experiment on the aircraft is also shown in Fig. 6.

During operation, lens commands are swept through and the resulting spot on a detector is imaged. Measurements are taken for 64 lens commands surrounding the focus, from 49.5 V to 53.5 V for the Corning Varioptic lens and 70 mA to 110 mA for the Optotune lens. The fastest data capture rate of every 300 ms and the 15-25 second parabola duration guide this quantity, with 64 points being approximately the number of points that can be captured in a single parabola, giving a complete sweep. The measured quantities include the image, acceleration (3-axis), gyro (3-axis), magnetometer (3-axis), and temperature. A flowchart of the software is shown in Fig. 5.

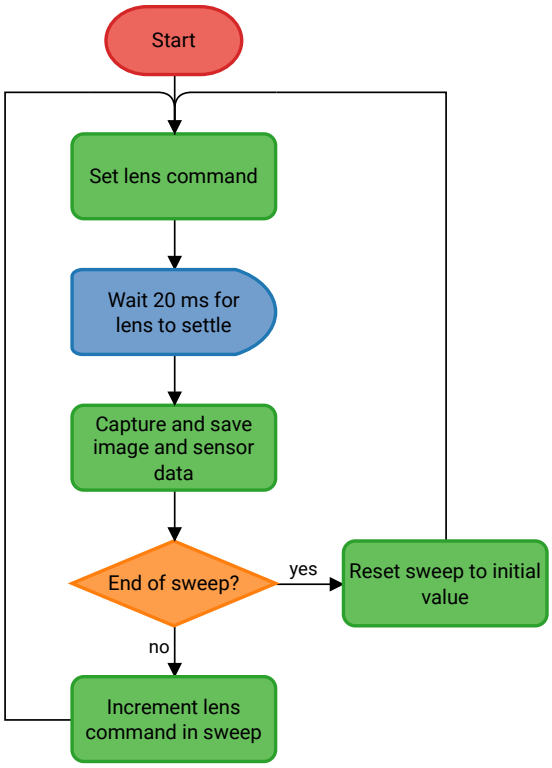

Fig 5: Flowchart of experiment flight software that runs continuously and records samples.

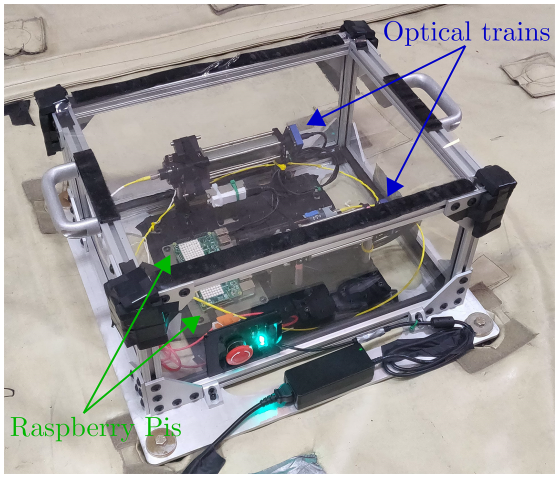

Fig 6: Experimental setup affixed to the floor of the zero gravity aircraft.

3.2 Spot Analysis

Using the data, the imaged spots on the detector can be analzyed to understand operational differences between the gravity regimes. As the beams deform significantly between gravity regimes, fitting standard Gaussian beams to understand how beam width varies is difficult. Instead, a metric for the relative spot width is used as shown in Equation 1, which is the square root of the number of pixels above an intensity threshold, can be used as a proxy for beam diameter. The limitations of this metric are that while it cannot be used for absolute beam width measurements, it can be used to understand relative changes.

With the threshold set to just above the noise floor of the sensor, this measurement should vary hyperbolically, in the same way that absolute beam diameter would.

$$r_{\text{spot}} = \sqrt{\text{n. pixels above threshold}} \quad (1)$$

4 Results and Discussion

In this section, measurements from the flight are used to understand how lens performance changes between zero gravity, Earth gravity, and hypergravity conditions. The spot analysis approach is used to understand how the lenses change in focal length and centroiding is used to determine how the point spread functions (PSFs) change in location for each condition.

4.1 Flight Profile and Measurements

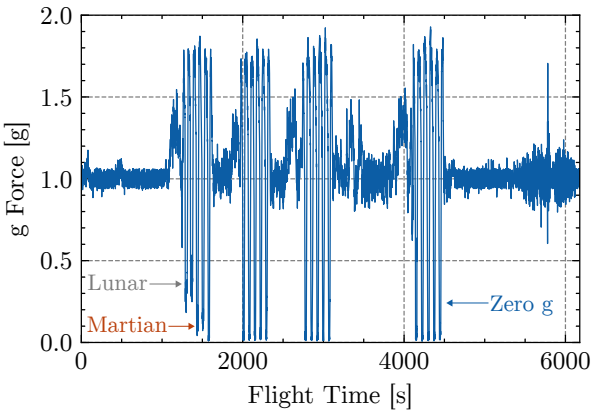

Fig 7: Complete parabolic flight profile of g-force against time showing takeoff, landing, and full 20 parabolas.

The flight profile of the experiment is shown in Fig. 7. The profile shows all 20 parabolas,

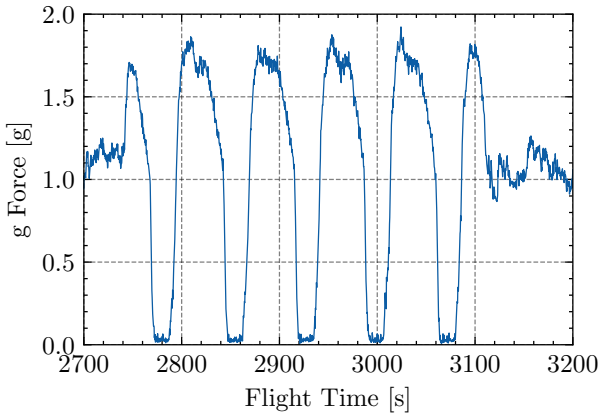

Fig 8: Zoomed view of g-force magnitude over time for second set of five parabolas. All parabolas in this set are zero gravity parabolas.

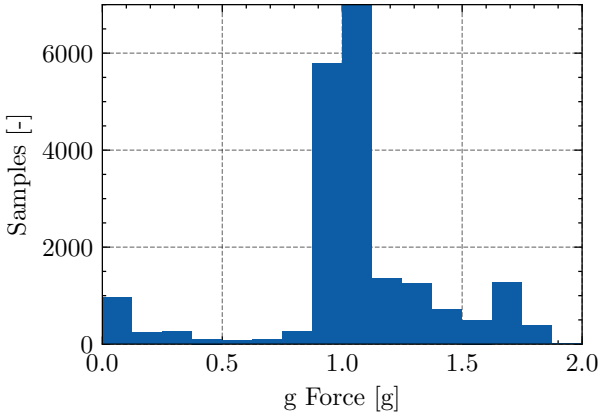

Fig 9: Histogram of total samples with g-force of each sample.

including the two parabolas each in Lunar and Martian gravity. The takeoff and landing phases are also clearly visible. Fig. 8 shows a zoomed in view of the second set of five parabolas.

Measurements of hypergravity experienced during the ascent phases of each parabola are also recorded, providing additional data for comparison. A histogram of the recorded g-force for all samples is shown in Table 9. Approximately 20,000 samples were collected for both Corning Varioptic and Optotune lenses.

4.2 Spot Analysis

Fig. 10 and Fig. 11 show individual focused samples from each gravity regime for the Corning Varioptic and Optotune lenses, respectively. As a first comparison, the Corning Varioptic focused spots have much smaller increases in tip/tilt and coma compared to the Optotune ones. The Optotune samples show very pronounced coma and deformation in higher gravity regimes. Some minor reflections are also visible for both Corning Varioptic and Optotune samples, although much more visible for the former than the latter.

The results for relative spot width over various lens commands are shown in Fig. 12 and Fig. 13. Overall, the analysis shows consistent results for both microgravity and Earth gravity with a few key differences. Both lenses show marginally increased focal length for the same lens command, and slightly lower relative spot width around the focal point. The increased focal length could be due to gravity providing some resistance to the actuation force that gets transferred horizontally due to surface tension on the lenses, whereas the smaller relative spot width is most likely due to lower aberrations in microgravity causing less smearing of the lens command. Lens focusing power increased in microgravity by 0.059 D for the Corning Varioptic A-39N0 and 0.039 D for the Optotune EL-16-40-TC-VIS lenses.

The Optotune lenses have well-constrained and consistent error bars throughout the lens commands, but the Corning Varioptic lenses show much larger error bars across the extremes of the sweep. This increased error caused the hyperbolic fits to be constrained towards the central section of points. The deviation seems due to variation in the samples causing parts of the image to pass below the threshold for relative spot width. Examples of samples at the same lens command but with different relative spot widths are shown in Fig. 14 and Fig. 15. An interesting defocus pattern from the Corning Varioptic lens forms, which then appears to be smeared, causing the high value for relative spot width in Fig. 14. The cause of this smearing is not obvious, but could be due to vibration of the liquid lens during the flight. There is no significant cor-

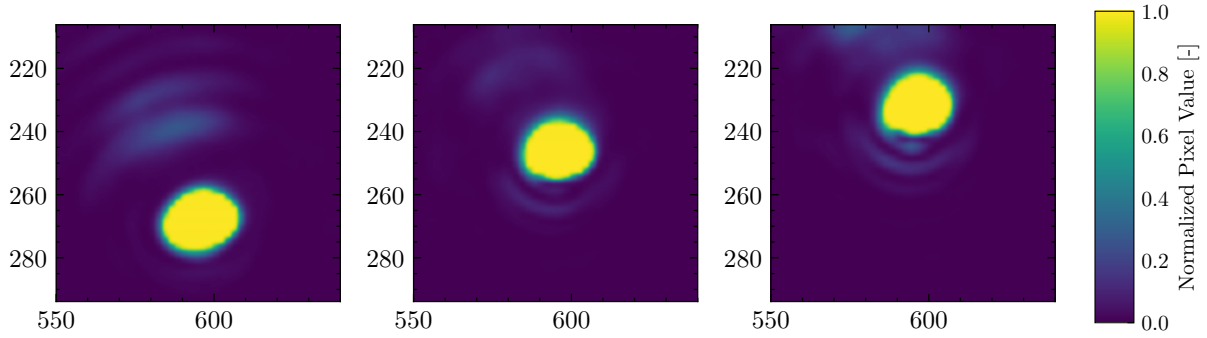

(a) 0g (b) 1g (c) 1.5g+ (d) Colorbar

Fig 10: Normalized images of focused individual Corning Varioptic samples from each gravity regime. Increasing gravity shows minor increases in tip/tilt and coma.

relation of this smearing to particular times of the flight or parabola. Some of the vibration also appears to make its way into the image as a result of circular standing waves, visible in the center of both Fig. 14 and Fig. 15.

4.3 Centroid Analysis

Fig. 16 and Fig. 17 show stacked and averaged images of the spot on the detector taken at each of their focal commands. The dominant aberration present is tip/tilt, with large changes between each gravity regime as summarized in Table 2 and measured using centroiding the PSFs from each lens. The change in tip/tilt is linear with the effect of gravity, with the linear regression shown in Fig. 18 and Fig. 19 for the Corning Varioptic and Optotune lenses respectively. Both sets of lenses adhere well to the linear fit, with an R^2 value of 0.78 for the Corning Varioptic lenses and 0.97 for the Optotune lenses. The R^2 value for the Corning Varioptic lenses is likely larger due to the smaller focused spot on the detector and the resulting increase in quantization noise when centroiding the PSF.

Qualitatively, it can also be seen in Fig. 10 and Fig. 11 that coma and astigmatism are also present, especially in hypergravity regimes. Corning Varioptic lenses exhibit less change in tip/tilt and maintain nearly identical optical performance. Optotune lenses show a larger change in tip/tilt, with significant coma observed in the hypergravity regime, as shown in Fig. 17.

The imaged PSFs for the Corning Varioptic lenses are well-contained, with no observable spread in hypergravity as compared to microgravity. The spots for the Optotune lenses are more spread out, suggesting that vibration or other environmental factors may have impacted the experiment and contributed to the observed aberrations. However, the imaged spots look visually tighter in microgravity, suggesting that there may be a gravity-dependent effect. The presence of more fluid in Optotune lenses may be a contributing factor to their optical performance being more significantly affected by environmental conditions. A an idealized diagram showing how fluid deformation could cause the resultant aberrations is shown in Fig. 20, although in reality, there would still be some minor fluid curvature at 0 g conditions due to surface tension.

Table 2: Change in tip/tilt of centroided spots for each regime, referenced to 0 g as a baseline.

Regime	**Tip/Tilt [mrad]**	
	Corning Varioptic	**Optotune**
1 g	0.79	4.13
1.5+ g	1.29	6.31

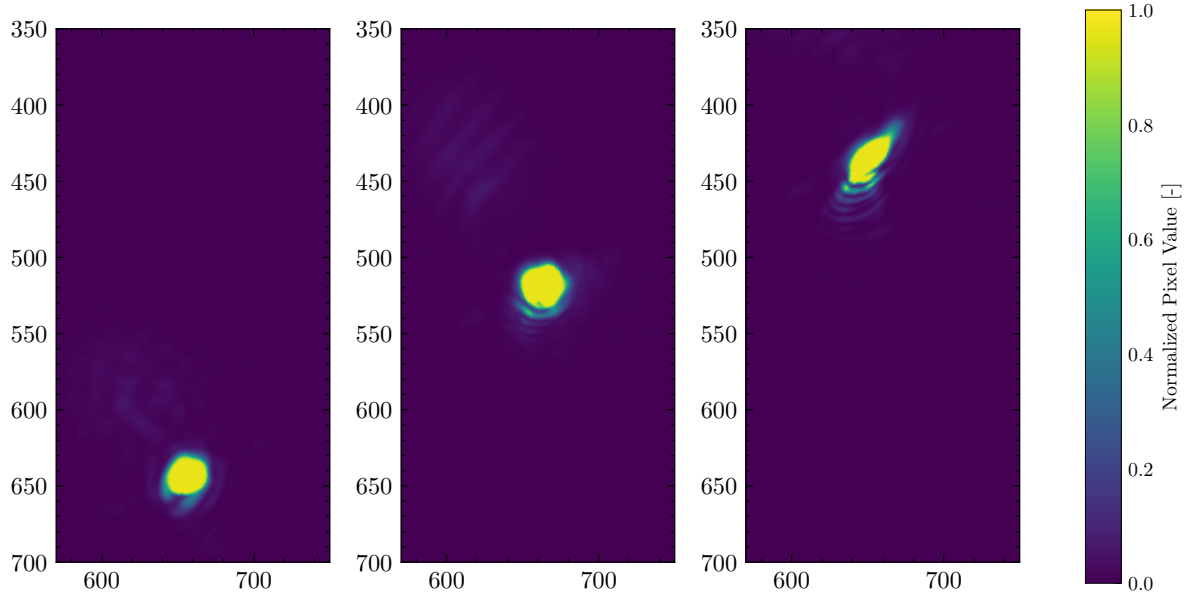

(a) 0g (b) 1g (c) 1.5g+ (d) Colorbar

Fig 11: Normalized images of focused individual Optotune samples from each gravity regime. Increases in gravity show larger increases in tip/tilt, coma, and smearing as compared to Fig. 10.

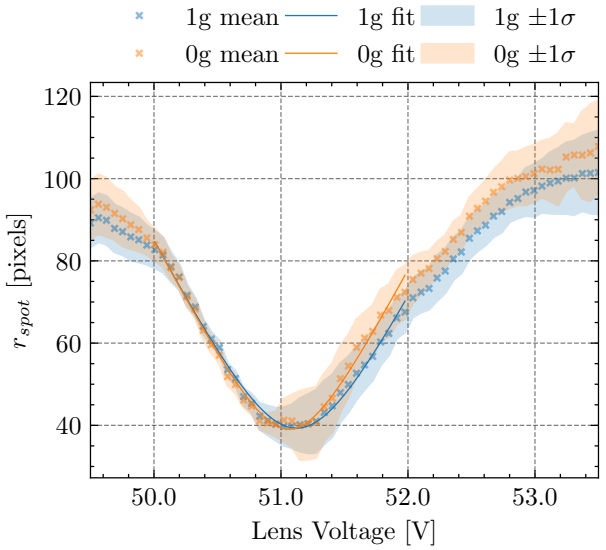

Fig 12: Relative spot width for sweep of lens commands for Corning Varioptic lenses, with associated hyperbolic fit and error bars.

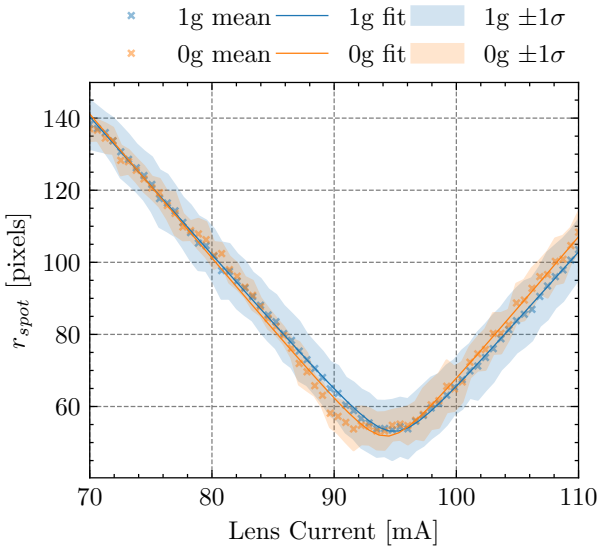

Fig 13: Relative spot width for sweep of lens commands for Optotune lenses, with associated hyperbolic fit and error bars.

4.4 Temperature Drift

Both liquid lenses used in this experiment have been shown to drift in focal length due to temperature variations. A temperature plot for both lenses as shown in Fig. 21 indicates that temperature throughout the parabolas was within 4 °C for all of the parabolas, with a gradual decrease after the lenses reached the peak temperature, as measured on the Raspberry Pi SenseHat modules. The Optotune temperature was slightly higher

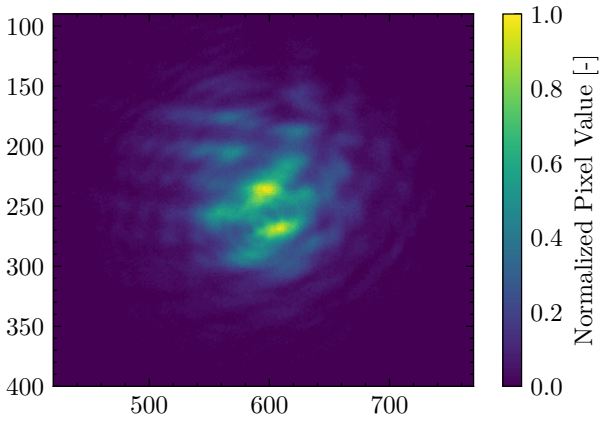

Fig 14: Example Corning Varioptic sample at 53.5 V lens voltage with high relative spot width caused by smeared features.

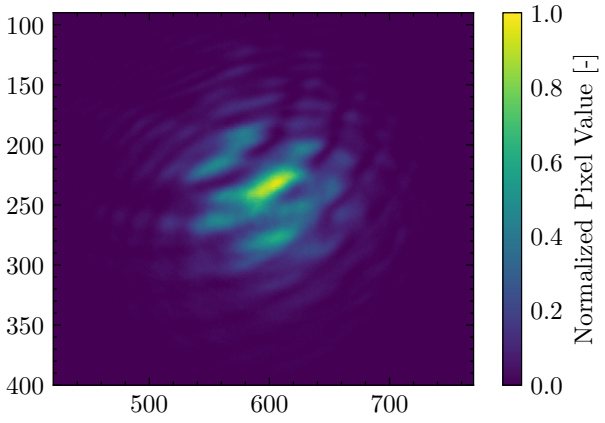

Fig 15: Example Corning Varioptic sample with low relative spot width, with identical lens command and gravity conditions as Fig. 14

than the Corning temperature during the flight, which is expected as Optotune lenses generate heat from their voice coil and high current operation. Histograms as shown in Fig. 22 and Fig. 23 reveal that a vast majority (75%) of the 0 g and 1 g data points are in the same range, effectively controlling for temperature drift during the experiment. Moreover, hypergravity and zero gravity data are comparable since temperature histograms are almost identical, indicating that the temperature is adequately controlled during the experiment. Interestingly, microgravity parabolas can be observed in the temperature plot, perhaps due to hydrostatic forces when transitioning into hypergravity causing redistribution of air inside the aircraft cabin.

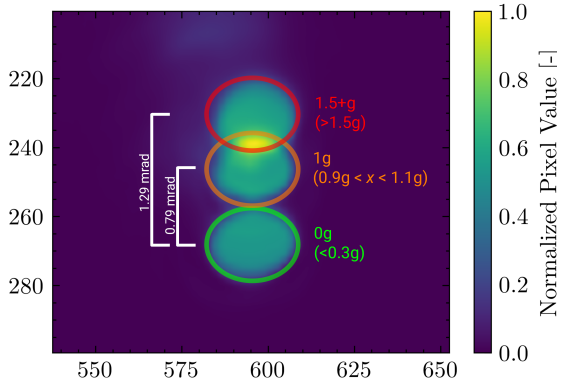

Fig 16: Image of stacked and averaged spots for each gravity environment for Corning Varioptic lenses (n: 0 g = 20, 1 g = 206, 1.5+ g = 37).

5 Conclusions and Future Work

This work shows that liquid lenses perform well in microgravity, with reduced overall aberrations, slight change in focusing behaviour and a change in tip/tilt. A summary of the quantitative results is shown in Table 3. A more pronounced disparity in operation is evident for Optotune lenses as compared with Corning Varioptic lenses, which is likely due to their larger aperture size holding more fluid volume.

During the microgravity flight, changes in temperature were small and limited to approximately 10 °C in the worst case. Prior studies have also shown that such fluctuations do not have a significant influence on the results.[1,2]

In combination with previous work on space environment evaluation,[1,2,5] these results show that liquid lenses are well suited for space-based optical systems. Their low SWaP-C and improved performance in microgravity in addition to previously studied operation in thermal vacuum and ionizing radiation effects make them a suitable option for use in a variety of space-related applications.[5]

Future work includes evaluating different control schemes in order to do closed-loop pointing

Table 3: Summary of changes in quantitatively determined properties of lenses, referenced to 0 g as a baseline.

Property	**Units**	**Change from 0 g to 1 g**	
		Corning Varioptic	**Optotune**
Tip/Tilt	mrad	0.79	4.13
Focal Length	Dioptres	-0.059	-0.039

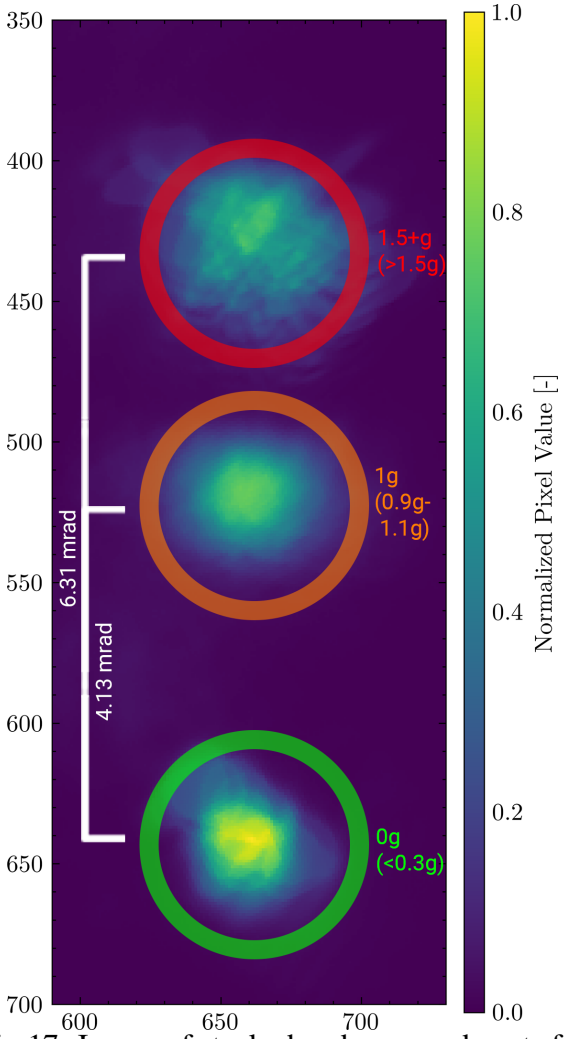

Fig 17: Image of stacked and averaged spots for each gravity environment for Optotune lenses (n: 0 g = 17, 1 g = 164, 1.5+ g = 26).

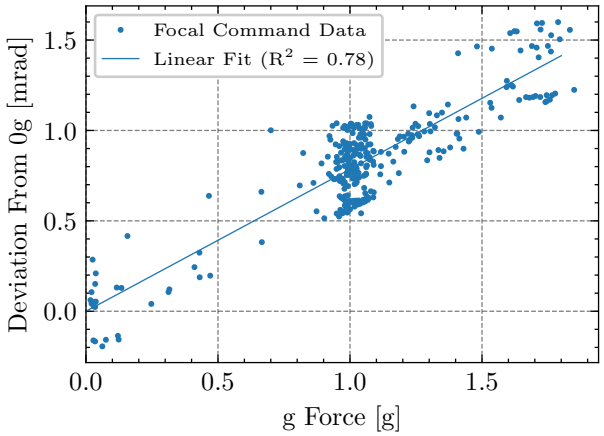

Fig 18: Linear regression of tip/tilt of focused samples against sample gravity conditions.

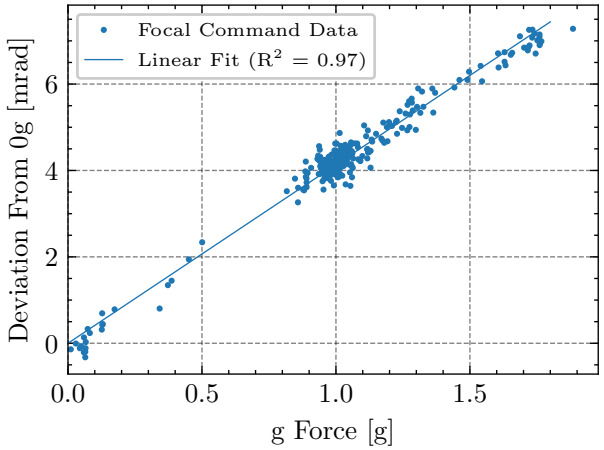

Fig 19: Linear regression of tip/tilt of focused samples against sample gravity conditions.

and tracking, as well as to compensate for the change in tip/tilt in different gravity conditions.

Further study of vibrations is needed, utilizing a vibrometer or faster IMU readout due to effects in smeared data points. With the data taken in this experiment, vibration could potentially be quantified using some of the resultant standing waves observed on the sample images.

Additionally, wavefront error is not evaluated in this study, as a wavefront sensor was not used during the microgravity flight. Evaluating the wavefront error using phase retrieval algorithms such as the Gerchberg-Saxton[16] algorithm, Mis-

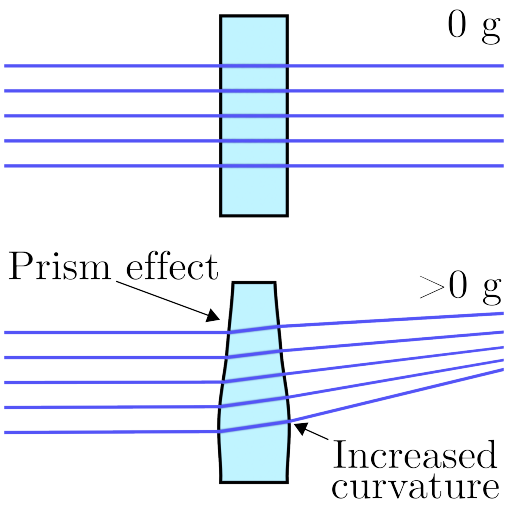

Fig 20: Potential physical mechanism explaining observed aberrations. Optical fluid sags to the bottom of the enclosure, causing slants in the side, which causes tip/tilt like a prism. Additionally, fluid curvature on the optical membrane creates higher order aberrations, such as coma and astigmatism.

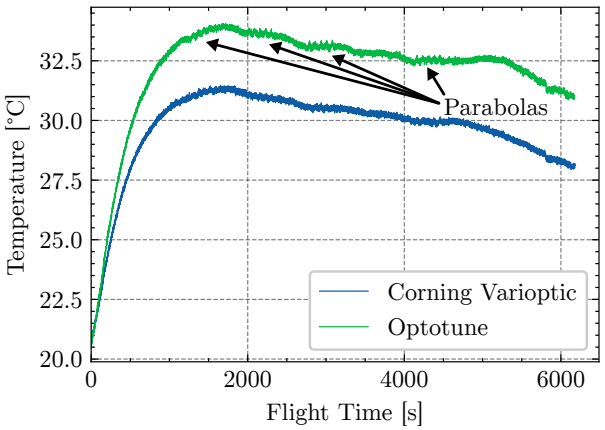

Fig 21: Temperature profile recorded on Raspberry Pi hat throughout flight. Optotune lenses due to their self heating have a higher temperature throughout the flight. Additionally, each parabola can be seen to have a very small impact on recorded temperature.

ell's algorithm,[17] and other nonlinear phase retrieval methods were attempted, but this process resulted in too much error and difficulty in convergence to obtain usable results.

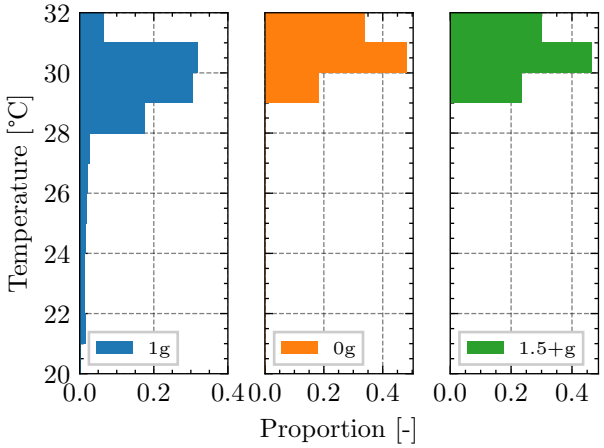

Fig 22: Histogram of temperatures for samples of Corning Varioptic lenses in all gravity conditions, showing that the majority of samples across all regimes are in the 29 °C to 30 °C range.

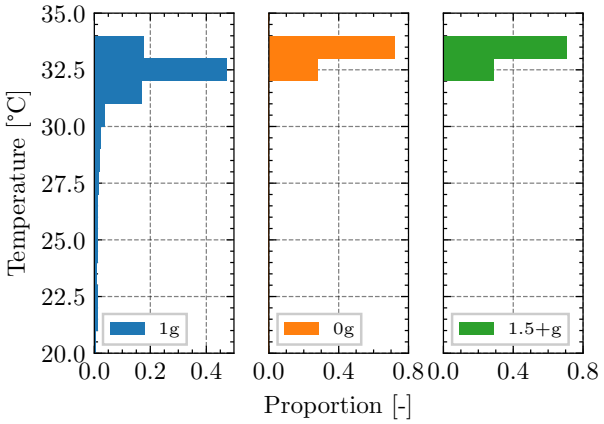

Fig 23: Histogram of temperatures for samples of Optotune lenses in all gravity conditions, showing that the majority of samples across all regimes are in the 32 °C to 34 °C range.

Disclosures

The authors declare that they have no conflicts of interest relevant to the content of this article.

Code, Data, and Materials Availability

Code and instructions for accessing data are available at this URL: https://github.com/MIT-STARLab/mosaic-zerog-code.

Acknowledgments

This work was supported by Early Stage Innovations grant 80NSSC19K0217 from NASA's Space Technology Research Grants Program. The authors would like to thank Dr. Sarah Tedder at NASA Glenn Research Center for her support and correspondence over the course of the program.

The authors would also like to thank Ariel Ekblaw, Sean Auffinger, and the rest of the MIT Media Lab Space Exploration Initiative for their support in organizing the zero gravity flight. Additionally, the authors appreciate the work of Mary Dahl and Maxwell Shepherd for help preparing documentation.

References

1 F. A. F. A. Fogle, *Liquid lens beam steering and environmental testing for the miniature optical steered antenna for inter-satellite communication*. Thesis, Massachusetts Institute of Technology (2020). Accepted: 2020-09-03T17:45:43Z.

2 F. Fogle, O. Cierny, P. d. V. Pereira, *et al.*, "Miniature Optical Steerable Antenna for Intersatellite Communications Liquid Lens Characterization," in *2020 IEEE Aerospace Conference*, 1–13 (2020). ISSN: 1095-323X.

3 "Optotune EL-16-40-TC manual."

4 S. Kacker, O. Cierny, J. Boyer, *et al.*, "Link analysis for a liquid lens beam steering system, the miniature optical steered antenna for intersatellite communication: MOSAIC," in *Free-Space Laser Communications XXXIII*, **11678**, 144–163, SPIE (2021).

5 S. Kacker, *Optical Performance and Prototyping of a Liquid Lens Laser Communications Transceiver*. Thesis, Massachusetts Institute of Technology (2022). Accepted: 2022-09-26T19:42:18Z.

6 M. Zohrabi, R. H. Cormack, and J. T. Gopinath, "Wide-angle nonmechanical beam steering using liquid lenses," *Optics Express* **24**, 23798–23809 (2016). Publisher: Optical Society of America.

7 "Corning Varioptic Lens Brochure."

8 J. Schneider, "The First Smartphone to Use a Liquid Lens is the Xiaomi Mi Mix Fold," (2021).

9 C. Efstathiou and V. M. Draviam, "Electrically tunable lenses – eliminating mechanical axial movements during high-speed 3D live imaging," *Journal of Cell Science* **134**, jcs258650 (2021).

10 V. Mai and H. Kim, "Variable Focus Lens-Based Beam Steering and Divergence Control for WDM Free-Space Optical Communication," in *Optical Fiber Communication Conference (OFC) 2022 (2022), paper M1C.6*, M1C.6, Optica Publishing Group (2022).

11 V. Mai and H. Kim, "Optical Beam Control Based on Variable Focus Lenses for WDM FSO Communications," in *2022 Conference on Lasers and Electro-Optics (CLEO)*, 1–2 (2022). ISSN: 2160-8989.

12 S. A. Reza and N. A. Riza, "A liquid lens-based broadband variable fiber optical attenuator," *Optics Communications* **282**, 1298–1303 (2009).

13 N. A. Riza and P. J. Marraccini, "Power smart in-door optical wireless link applications," in *2012 8th International Wireless Communications and Mobile Computing Conference (IWCMC)*, 327–332 (2012). ISSN: 2376-6506.

14 N. A. Riza, "Smart Optical Beamforming for Next Generation Wireless Empowered Communications, Power Transfer, Sensing and Displays: Building on the Past," in *2022 33rd Irish Signals and Systems Conference (ISSC)*, 1–7 (2022). ISSN: 2688-1454.

15 V. V. Mai and H. Kim, "Non-Mechanical Beam Steering and Adaptive Beam Control Using Variable Focus Lenses for Free-Space Optical Communications," *Journal of Lightwave Technology* **39**, 7600–7608 (2021). Conference Name: Journal of Lightwave Technology.

16 R. W. Gerchberg and W. O. Saxton, "A Practical Algorithm for the Determination of Phase from Image and Diffraction Plane Pictures," *Optik* **35**, 6 (1972).

17 D. L. Misell, "A method for the solution of the phase problem in electron microscopy," *Journal of Physics D: Applied Physics* **6**, L6–L9 (1973).

Shreeyam Kacker is a graduate student in the MIT Space Telecommunications, Astronomy, and Radiation Laboratory led by Prof. Kerri Cahoy. He received the SM degree from MIT in Aeronautics and Astronautics in 2022, and the MEng degree in Aeronautical Engineering from Imperial College London in 2020. His research specializes in laser communications and machine learning applied to remote sensing.

List of Figures

List of Tables